Probing neutrino magnetic moments at the Spallation Neutron Source facility

T. S. Kosmas,[1,*] O. G. Miranda,[2,†] D. K. Papoulias,[1,3,‡] M. Tórtola,[3,§] and J. W. F. Valle[3,‖]

[1]*Theoretical Physics Section, University of Ioannina, GR-45110 Ioannina, Greece*
[2]*Departamento de Física, Centro de Investigación y de Estudios Avanzados del IPN, Apartado Postal 14-740 07000, Distrito Federal, Mexico*
[3]*AHEP Group, Instituto de Física Corpuscular–C.S.I.C./Universitat de València Edificio de Institutos de Paterna, C/Catedratico José Beltrán, 2 E-46980 Paterna (València), Spain*

(Received 19 May 2015; published 20 July 2015)

Majorana neutrino electromagnetic properties are studied through neutral current coherent neutrino-nucleus scattering. We focus on the potential of the recently planned COHERENT experiment at the Spallation Neutron Source to probe muon-neutrino magnetic moments. The resulting sensitivities are determined on the basis of a χ^2 analysis employing realistic nuclear structure calculations in the context of the quasiparticle random phase approximation. We find that they can improve existing limits by half an order of magnitude. In addition, we show that these facilities allow for standard model precision tests in the low energy regime, with a competitive determination of the weak mixing angle. Finally, they also offer the capability to probe other electromagnetic neutrino properties, such as the neutrino charge radius. We illustrate our results for various choices of experimental setup and target material.

DOI: 10.1103/PhysRevD.92.013011 PACS numbers: 13.15.+g, 14.60.St, 12.60.-i, 13.40.Em

I. INTRODUCTION

The robust confirmation of the existence of neutrino masses and mixing [1,2], thanks to the milestone discovery of neutrino oscillations in propagation from solar, atmospheric, accelerator, and reactor neutrino sources, has opened a window to probe new physics beyond the standard model (SM) (for the relevant experimental references see, e.g., [3,4]). While the ultimate origin of neutrino mass remains a mystery [5], oscillation results have motivated a plethora of SM extensions to generate small neutrino masses [6]. A generic feature of such models is the existence of nontrivial neutrino electromagnetic (EM) properties [7–12]. Although the three-neutrino oscillation paradigm seems to be on rather solid ground [13,14], nontrivial neutrino electromagnetic properties may still play an important subleading role in precision neutrino studies [15].

The lowest-order contribution of neutrino EM interactions involves neutrino magnetic moments (NMM) [11,16,17], as well as the neutrino charge radius [18–20] arising from loop-level radiative corrections [21,22]. Note that a direct neutrino magnetic moment measurement could provide a key insight in the understanding of the electroweak interactions, and the Majorana nature of neutrinos [23,24]. Indeed, in contrast to the case of Majorana neutrinos, only massive Dirac neutrinos can have nonvanishing diagonal magnetic moments [7,9,10,12]. In the general Majorana case, only off-diagonal transition magnetic moments exist; they form an antisymmetric matrix, calculable from first principles, given the underlying gauge theory.

Within the minimally extended $\mathrm{SU(3)_c} \otimes \mathrm{SU(2)_L} \otimes \mathrm{U(1)_Y}$ model with Dirac neutrino masses, one expects tiny NMM, of the order of $\mu_\nu \leq 10^{-19}\mu_B(\frac{m_\nu}{1\ \mathrm{eV}})$, expressed in Bohr magnetons μ_B [25,26]. However, appreciably larger Majorana neutrino transition magnetic moments are expected in many theoretical models, such as those involved with left-right symmetry [27], scalar leptoquarks [28], R-parity-violating supersymmetry [29], and large extra dimensions [30]. Currently, the most stringent upper limits, $\mu_\nu \leq \text{few} \times 10^{-12}\mu_B$, come from astrophysics [16,17,31,32]. In addition, there are bounds from measurements by various terrestrial neutrino scattering experiments. The present status of such constraints is summarized in Table I where one can see that the direct constraints on μ_{ν_μ} and μ_{ν_e} are still rather poor. It should be mentioned, however, that currently operating reactor

TABLE I. Summary of the current 90% C.L. constraints on neutrino magnetic moments from various experiments.

Experiment	Reaction	Observable	Constraint ($10^{-10}\mu_B$)
LSND [33]	$\nu_\mu e^- \to \nu_\mu e^-$	μ_{ν_μ}	6.8
LAMPF [34]	$\nu_e e^- \to \nu_e e^-$	μ_{ν_e}	10.8
TEXONO [35]	$\bar{\nu}_e e^- \to \bar{\nu}_e e^-$	$\mu_{\bar{\nu}_e}$	0.74
GEMMA [36]	$\bar{\nu}_e e^- \to \bar{\nu}_e e^-$	$\mu_{\bar{\nu}_e}$	0.29

*hkosmas@uoi.gr
†omr@fis.cinvestav.mx
‡dimpap@cc.uoi.gr
§mariam@ific.uv.es
‖valle@ific.uv.es

neutrino experiments such as TEXONO and GEMMA have set robust constraints on $\mu_{\bar{\nu}_e}$.

The possibility of probing neutrino EM parameters, such as the NMM and the neutrino charge radius, through coherent elastic neutrino-nucleus scattering (CENNS) [37,38] can be explored on the basis of a sensitivity χ^2-type analysis [39–45]. To this end we perform realistic nuclear structure calculations [46,47] in order to compute accurately the relevant cross sections [48–50]. The required proton and neutron nuclear form factors are reliably obtained within the context of the quasiparticle random phase approximation (QRPA) method by considering realistic strong nuclear forces [51–54]. Concentrating on ongoing and planned neutrino experiments, we have devoted special effort in estimating the expected number of CENNS events with high significance. Specifically, our study is focused on the proposed detector materials of the COHERENT experiment [55,56] at the Spallation Neutron Source (SNS) [57]. Even though a CENNS event has never been experimentally measured, we remark that the highly intense neutrino beams [58,59] provided at the SNS indicate very encouraging prospects towards the detection of this reaction for the first time [60,61], by using low energy detectors [62]. Furthermore, neutrinos from stopped pion-muon beams [63,64] at the SNS [65,66] or elsewhere [67,68] have motivated many studies searching for physics beyond the SM model, too [43,50,69,70].

In the present work we quantify the prospects, not only of detecting CENNS events at the SNS, but also of performing precision electroweak measurements and probing neutrino properties beyond the SM. We conclude that the extracted sensitivities on the effective NMM improve with respect to previous results of studies of this type. We obtain for the first time robust upper limits on μ_{ν_μ}. Moreover, we obtain a sensitivity for the neutrino charge radius, which is competitive with those of previous studies. Furthermore, we explore the sensitivity of these experiments for standard model precision measurements of the weak mixing angle in the energy regime of a few MeV.

II. COHERENT ELASTIC NEUTRINO-NUCLEUS SCATTERING

The CENNS is described within the SM starting from the neutrino-quark neutral-current (NC) interaction, but is expected to have corrections coming from new physics [3], such as nonstandard interactions [39,41–45,49,50] or nontrivial neutrino electromagnetic properties [70]. Here we focus on the latter [16,17,20].

A. Standard model prediction

At low and intermediate neutrino energies $E_\nu \ll M_W$, the weak neutral-current cross section describing this process in the SM is given by the four-fermion effective interaction Lagrangian, $\mathcal{L}_{\rm SM}$,

$$\mathcal{L}_{\rm SM} = -2\sqrt{2}G_F \sum_{\substack{f=u,d \\ \alpha=e,\mu,\tau \\ P=L,R}} g_{\alpha\alpha}^{f,P}[\bar{\nu}_\alpha \gamma_\rho L \nu_\alpha][\bar{f}\gamma^\rho P f], \quad (1)$$

where $P = \{L, R\}$ are the chiral projectors, $\alpha = \{e, \mu, \tau\}$ denotes the neutrino flavor, f is a first generation quark, and G_F is the Fermi constant. The left- and right-hand coupling constants for the u- and d-quark to the Z-boson including the relevant radiative corrections are given as [15]

$$\begin{aligned} g_{\alpha\alpha}^{u,L} &= \rho_{\nu N}^{\rm NC}\left(\frac{1}{2} - \frac{2}{3}\hat{\kappa}_{\nu N}\hat{s}_Z^2\right) + \lambda^{u,L}, \\ g_{\alpha\alpha}^{d,L} &= \rho_{\nu N}^{\rm NC}\left(-\frac{1}{2} + \frac{1}{3}\hat{\kappa}_{\nu N}\hat{s}_Z^2\right) + \lambda^{d,L}, \\ g_{\alpha\alpha}^{u,R} &= \rho_{\nu N}^{\rm NC}\left(-\frac{2}{3}\hat{\kappa}_{\nu N}\hat{s}_Z^2\right) + \lambda^{u,R}, \\ g_{\alpha\alpha}^{d,R} &= \rho_{\nu N}^{\rm NC}\left(\frac{1}{3}\hat{\kappa}_{\nu N}\hat{s}_Z^2\right) + \lambda^{d,R}, \end{aligned} \quad (2)$$

with $\hat{s}_Z^2 = \sin^2\theta_W = 0.23120$, $\rho_{\nu N}^{\rm NC} = 1.0086$, $\hat{\kappa}_{\nu N} = 0.9978$, $\lambda^{u,L} = -0.0031$, $\lambda^{d,L} = -0.0025$, and $\lambda^{d,R} = 2\lambda^{u,R} = 7.5 \times 10^{-5}$.

Since neutrino detection experiments are sensitive to the kinetic energy of the recoiling nucleus, one expresses the differential cross section accordingly. Using the effective Lagrangian of Eq. (1), one can describe the coherent neutrino scattering off a spherical spin-zero nucleus of mass M by computing the differential cross section with respect to the nuclear recoil energy, T, as [49,50]

$$\left(\frac{d\sigma}{dT}\right)_{\rm SM} = \frac{G_F^2 M}{\pi}\left(1 - \frac{MT}{2E_\nu^2}\right)|\langle gs||\hat{\mathcal{M}}_0(q)||gs\rangle|^2, \quad (3)$$

where E_ν is the neutrino energy. Within the context of the Donnelly-Walecka multipole decomposition method, the relevant nuclear matrix element for the dominant coherent channel ($gs \to gs$ transitions) is based on the Coulomb operator $\hat{\mathcal{M}}_0$ [51]. The latter is a product of the zero-order spherical Bessel function times the zero-order spherical harmonic [48,52–54] and can be cast in the form [49]

$$\begin{aligned} |\mathcal{M}_V^{\rm SM}|^2 &\equiv |\langle gs||\hat{\mathcal{M}}_0(q)||gs\rangle|^2 \\ &= [g_V^p Z F_Z(q^2) + g_V^n N F_N(q^2)]^2. \end{aligned} \quad (4)$$

The finite nuclear size is taken into account by expressing the Coulomb matrix element in terms of the proton (neutron) nuclear form factors $F_{Z(N)}(q^2)$, reflecting the dependence of the coherent rate on the variation of the momentum transfer, $q^2 \simeq 2MT$. The polar-vector couplings of protons (g_V^p) and neutrons (g_V^n) to the Z-boson are defined as $g_V^p = 2(g_{\alpha\alpha}^{u,L} + g_{\alpha\alpha}^{u,R}) + (g_{\alpha\alpha}^{d,L} + g_{\alpha\alpha}^{d,R})$ and $g_V^n = (g_{\alpha\alpha}^{u,L} + g_{\alpha\alpha}^{u,R}) + 2(g_{\alpha\alpha}^{d,L} + g_{\alpha\alpha}^{d,R})$, respectively. It can be noticed that the vector proton coupling, g_V^p, is small

compared to the corresponding neutron coupling, g_V^n; therefore, the dominant contribution to the coherent cross section scales with the square of the number of neutrons of the target isotope.

In this work we perform realistic nuclear structure calculations for the experimentally interesting even-even nuclear isotopes, ^{20}Ne, ^{40}Ar, ^{76}Ge, and ^{132}Xe. To this aim, the nuclear ground state, $|gs\rangle \equiv |0^+\rangle$, has been constructed by solving (iteratively) the BCS equations, quite precisely. In this framework, the proton (neutron) nuclear form factors read [46]

$$F_{N_n}(q^2) = \frac{1}{N_n}\sum_j \sqrt{2j+1}\langle j|j_0(qr)|j\rangle (v_{N_n}^j)^2, \qquad (5)$$

where $N_n = Z$ (or N) and $v_{N_n}^j$ denotes the occupation probability amplitude of the jth single-nucleon level. For each nuclear system, the chosen active model space, as well as the required monopole (pairing) residual interaction that was obtained from a Bonn C-D two-body potential (strong two-nucleon forces) and slightly renormalized with two parameters $g_{\rm pair}^{p(n)}$ for proton (neutron) pairs, has been taken from Ref. [50]. The above method has been successfully applied for similar calculations of various semileptonic nuclear processes [47,52,54].

B. Electromagnetic neutrino-nucleus cross sections

After the discovery of neutrino oscillations [13,14] over a decade ago, it became evident that neutrinos are indeed massive particles [1,2] and, as a result, they may acquire nontrivial electromagnetic properties as well [23,24]. At low-momentum transfer, the description of possible neutrino EM interactions involves two types of phenomenological parameters, the anomalous magnetic moment and the mean-square charge radius [7–12]. It is worth mentioning that the photon exchange involving a neutrino magnetic moment flips the neutrino helicity, while in the interaction due to the weak gauge boson exchange the helicity is preserved.

The electromagnetic neutrino-nucleus vertex has been comprehensively studied [26], and its contribution to the coherent elastic cross section including nuclear physics details takes the form [70]

$$\left(\frac{d\sigma}{dT}\right)_{\rm EM} = \frac{\pi\alpha_{\rm em}^2\mu_{\rm eff}^2 Z^2}{m_e^2}\left(\frac{1-T/E_\nu}{T}\right)F_Z^2(q^2), \qquad (6)$$

where $\alpha_{\rm em}$ is the fine structure constant and $\mu_{\rm eff}$ is the effective neutrino magnetic moment.

In this framework, the helicity preserving standard weak interaction cross section (SM) adds incoherently with the helicity-violating EM cross section, so the total cross section is written as

$$\left(\frac{d\sigma}{dT}\right)_{\rm tot} = \left(\frac{d\sigma}{dT}\right)_{\rm SM} + \left(\frac{d\sigma}{dT}\right)_{\rm EM}. \qquad (7)$$

The latter expression will be used below in order to constrain the effective neutrino magnetic moment parameters.

III. NEUTRINOS FROM THE SPALLATION NEUTRON SOURCE

There are several experimental proposals that plan to detect for the first time a CENNS [65–68] signal. In this section, we describe the ongoing COHERENT experiment [55,56], proposed to operate at the SNS at Oak Ridge National Lab [57]. This facility provides excellent prospects for measuring CENNS events for the first time. In general, any potential deviation from the SM expectations can be directly interpreted as a signature of new physics and, thus, has prompted many theoretical studies searching for physics within [60,61] and beyond the SM [40,41,43,50,69].

Currently, the SNS constitutes the leading facility for neutron physics searches, producing neutrons by firing a pulsed proton beam at a liquid mercury target [65]. In addition to neutrons, the mercury target generates pions, which decay producing neutrino beams as a free by-product. These beams are exceptionally intense, of the order of $\Phi = 2.5\times10^7\nu\ {\rm s}^{-1}\,{\rm cm}^{-2}$ ($\Phi = 6.3\times10^6\nu\ {\rm s}^{-1}\,{\rm cm}^{-2}$) per flavor at 20 m (40 m) from the spallation target [58]. In stopped pion-muon sources, a monoenergetic muon-neutrino ν_μ flux with energy 29.9 MeV is produced via pion decay at rest $\pi^+ \to \mu^+\nu_\mu$ within $\tau = 26$ ns (prompt flux), followed by electron neutrinos, ν_e, and muon antineutrinos, $\bar\nu_\mu$, that are emitted from the muon-decay $\mu^+ \to \nu_e e^+\bar\nu_\mu$ within $\tau = 2.2$ μs (delayed flux) [59]. The ν_e and $\bar\nu_\mu$ neutrino spectra are described at rather high precision by the normalized distributions [63,64]

$$\eta_{\nu_e}^{\rm SNS} = 96E_\nu^2 M_\mu^{-4}(M_\mu - 2E_\nu),$$
$$\eta_{\bar\nu_\mu}^{\rm SNS} = 16E_\nu^2 M_\mu^{-4}(3M_\mu - 4E_\nu), \qquad (8)$$

with maximum energy of $E_\nu^{\rm max} = M_\mu/2$ ($M_\mu = 105.6$ MeV is the muon rest mass).

In this work we distinguish two cases, the optimistic and the realistic ones. The first case is convenient for exploring the nuclear responses of different nuclear detector isotopes, in order to get a first idea of the relevant neutrino parameters within and beyond the SM. The second case is useful in quantifying the sensitivities attainable with various individual technologies of each experimental setup. Both cases are useful and complementary to illustrate the potential of the proposal. For instance, for the realistic case, the original COHERENT proposal considers different detectors to be located in different rooms and, therefore,

TABLE II. Summary of the detector concepts assumed in this work. We consider four possible nuclei as targets and two possible experimental setups for each nucleus: a realistic one, for different detector masses, distances, recoil energy windows, and efficiencies, and the optimistic case where all the variables are allowed to have their "best" value.

COHERENT experiment					
		^{20}Ne [55]	^{40}Ar [55]	^{76}Ge [69]	^{132}Xe [55,62]
Realistic	Mass	391 kg	456 kg	100 kg	100 kg
	Distance	46 m	46 m	20 m	40 m
	Efficiency	50%	50%	67%	50%
	Recoil window	30–160 keV	20–120 keV	10–78 keV	8–46 keV
Optimistic	Mass	1 ton	1 ton	1 ton	1 ton
	Distance	20 m	20 m	20 m	20 m
	Efficiency	100%	100%	100%	100%
	Recoil window	1 keV–$T_{\max}$	1 keV–$T_{\max}$	1 keV—$T_{\max}$	1 keV–$T_{\max}$

at different distances. In particular, the ^{132}Xe detector is considered to be 40 m from the source while other isotopes are expected to be 20 m. Clearly, for shorter distances the attainable sensitivities would be higher for any of these detectors; this possibility is considered in the optimistic case.

In our calculations, we assume a time window of one year for the optimistic case and 2.4×10^7 s for the realistic case [66]. Detailed information on the different detector setups considered here is summarized in Table II. For a comprehensive description of the relevant nuclear isotopes including the experimental criteria and advantages of adopting each of them, the reader is referred to Refs. [40,50].

IV. NUMERICAL RESULTS

Assuming negligible neutrino oscillation effects in short-distance propagation, for each interaction channel, $x = \mathrm{SM}, \mathrm{EM}, \mathrm{tot}$, the total number of counts above a certain threshold, T_{thres}, is given through the expression

$$N_x^{\mathrm{events}} = K \int_{E_{\nu_{\min}}}^{E_{\nu_{\max}}} \eta^{\mathrm{SNS}}(E_\nu) dE_\nu \int_{T_{\mathrm{thres}}}^{T_{\max}} \left(\frac{d\sigma}{dT}(E_\nu, T)\right)_x dT, \tag{9}$$

where $K = N_{\mathrm{targ}} t_{\mathrm{tot}} \Phi$, with N_{targ} being the total number of atomic targets in the detector, t_{tot} the time window of data taking, and Φ the total neutrino flux. In the present calculations, the various experimental concepts are taken into account by fixing the corresponding input parameters as discussed previously.

A. Standard model precision tests at SNS

We first examine the sensitivity of the COHERENT experiment to the weak mixing angle $\sin^2\theta_W$ of the SM in the low energy regime of the SNS operation. In order to quantify this sensitivity, assuming that the experimental proposal will measure exactly the SM prediction, we perform a statistical analysis based on a χ^2 with statistical errors only,

$$\chi^2 = \left(\frac{N_{\mathrm{SM}}^{\mathrm{events}} - N_{\mathrm{SNS}}^{\mathrm{events}}(\sin^2\theta_W)}{\delta N_{\mathrm{SM}}^{\mathrm{events}}}\right)^2, \tag{10}$$

where the number of SM events, $N_{\mathrm{SM}}^{\mathrm{events}}$, depends on the Coulomb nuclear matrix element entering the coherent rate. As the central value for the SM weak mixing angle prediction we adopt the Particle Data Group (PDG) value $\hat{s}_Z^2 = 0.23120$. We then compute the χ^2 function depending on the expected number of events for a given value of the mixing angle, $N_{\mathrm{SNS}}^{\mathrm{events}}(\sin^2\theta_W)$. The corresponding results for the various detector materials of the COHERENT experiment are shown in Fig. 1. In Table III, we illustrate the band, $\delta\sin^2\theta_W \equiv \delta s_W^2$, at 90% C.L. evaluated as $\delta s_W^2 = (s_{W^{\max}}^2 - s_{W^{\min}}^2)/2$ and the corresponding uncertainty $\delta s_W^2/\hat{s}_Z^2$, with $s_{W^{\max}}^2$ and $s_{W^{\min}}^2$ being the upper and lower 1σ error, respectively. At the optimistic level, our results indicate that better sensitivities are expected for heavier target nuclei, such as ^{132}Xe. This is understood as a direct consequence of the significantly larger number of expected events provided by heavier nuclear isotopes [50]. However, once we consider the realistic case, the expectations change drastically so that, for the case of a ^{76}Ge detector we find a better sensitivity, due to a closer location to the SNS source (20 m in comparison with the 40 m for the ^{132}Xe case) and a higher efficiency in recoil acceptance (see Table II). Furthermore, in Fig. 2 and Table IV, we show that the expected sensitivities improve through a combined measurement of the prompt and delayed beams ($\nu_\mu + \bar{\nu}_\mu$).

B. EM neutrino interactions at SNS

One of the main goals of our present work is to examine the sensitivity of the COHERENT experiment to the possible detection of CENNS events due to neutrino EM effects, associated with various effective transition NMM parameters such as $\mu_{\nu_\mu}, \mu_{\bar{\nu}_\mu}$, and μ_{ν_e}. The total number of

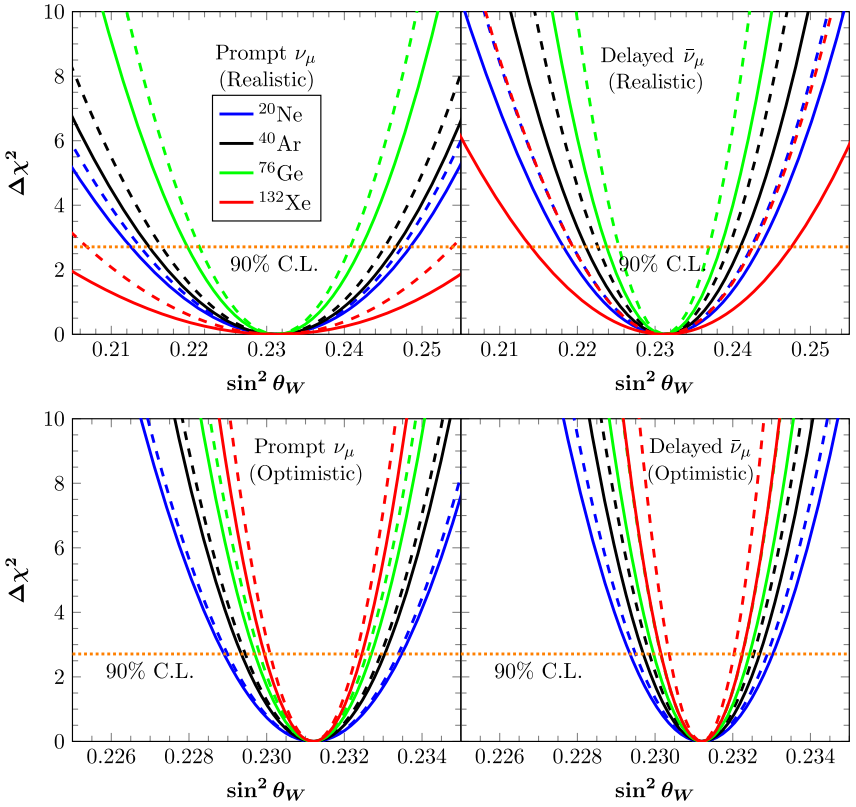

FIG. 1 (color online). $\Delta\chi^2$ profile in terms of the weak mixing angle $\sin^2\theta_W$ showing the sensitivity of the COHERENT experiment to SM precision tests. The PDG value $\hat{s}^2_Z = 0.23120$ is used as the central value. Left (right) panels illustrate the results obtained by considering the prompt (delayed) flux, while upper (lower) panels account for the realistic (optimistic) case. Here, the solid (dashed) lines refer to the nuclear BCS method (zero-momentum transfer).

events expected in an experiment searching for CENNS depends strongly on the energy threshold T_{thres} as well as the total mass of the detector. For low energy thresholds and more massive detectors, the total number of events expected is significantly larger and, therefore, the attainable constraints are more stringent. We remind the reader that, for a possible NMM detection, a very low energy threshold is required, since the EM cross section dominates at low energies.

The sensitivity is evaluated by assuming that a given experiment searching for CENNS events will measure exactly the SM expectation; thus any deviation is understood as a signature of new physics. Following [24] we define the χ^2 function as

$$\chi^2 = \left(\frac{N^{\text{events}}_{\text{SM}} - N^{\text{events}}_{\text{tot}}(\mu_{\nu_\alpha})}{\delta N^{\text{events}}_{\text{SM}}}\right)^2. \tag{11}$$

TABLE III. Expected sensitivities to the weak mixing angle $\sin^2\theta_W(\nu_\alpha) \equiv s^2_W(\nu_\alpha)$, assuming the various channels $(\nu_\mu, \bar{\nu}_\mu, \nu_e)$ of the SNS beam for a set of possible detectors at the COHERENT experiment. For the realistic (optimistic) case, the band $\delta s^2_W(\nu_\alpha)$ and the corresponding uncertainty are evaluated within 1σ error.

Nucleus	$\delta s^2_W(\nu_\mu)$	Uncertainty (%)	$\delta s^2_W(\bar{\nu}_\mu)$	Uncertainty (%)	$\delta s^2_W(\nu_e)$	Uncertainty (%)
^{20}Ne	0.0110	4.74	0.0077	3.33	0.0091	3.94
	[0.0014]	[0.61]	[0.0011]	[0.48]	[0.0013]	[0.56]
^{40}Ar	0.0097	4.17	0.0061	2.64	0.0074	3.20
	[0.0011]	[0.48]	[0.0009]	[0.39]	[0.0010]	[0.43]
^{76}Ge	0.0068	2.94	0.0045	1.92	0.0055	2.36
	[0.0009]	[0.39]	[0.0008]	[0.35]	[0.0009]	[0.37]
^{132}Xe	0.0181	7.83	0.0102	4.39	0.0127	5.47
	[0.0008]	[0.35]	[0.0006]	[0.26]	[0.0007]	[0.30]

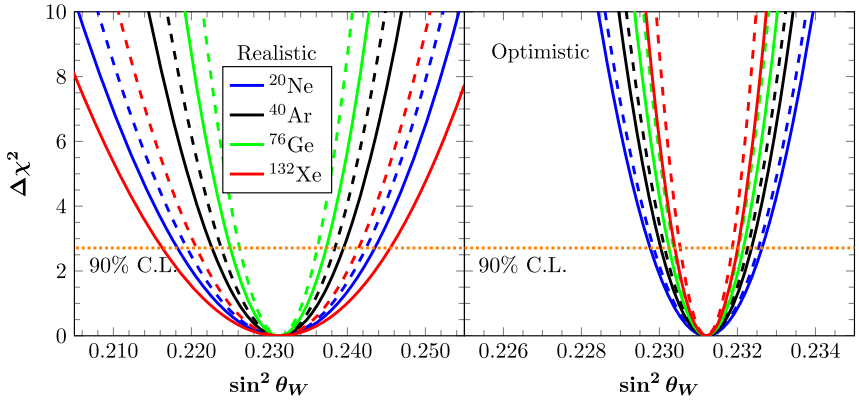

FIG. 2 (color online). $\Delta\chi^2$ profile in terms of the weak mixing angle $\sin^2\theta_W$ from the combined measurement of the prompt and delayed beams $(\nu_\mu + \bar{\nu}_\mu)$. The same conventions as in Fig. 1 are used.

By employing the aforementioned method, we find that the COHERENT experiment could provide useful complementary limits on μ_{ν_μ}. On the other hand, the sensitivity to μ_{ν_e} is not expected to be as good as that of reactor experiments [35,36]. However, a combined analysis of the prompt and delayed muon-neutrino beams $(\nu_\mu + \bar{\nu}_\mu)$ could help to further improve the sensitivity to a neutrino magnetic moment. The same applies to the combination of different detectors using the same neutrino source. For different nuclear targets, the present results are shown in Figs. 3–4 and the sensitivities on neutrino magnetic moments at 90% C.L. are summarized in Table V.

The sensitivity to neutrino magnetic moments has also been computed for the case of a combined measurement with different target nuclei. In this framework, we take advantage of the multitarget strategy of the COHERENT experiment [55,56] and define the χ^2 as

$$\chi^2 = \sum_{\text{nuclei}} \left(\frac{N_{\text{SM}}^{\text{events}} - N_{\text{tot}}^{\text{events}}(\mu_{\nu_\alpha})}{\delta N_{\text{SM}}^{\text{events}}} \right)^2. \tag{12}$$

Assuming two nuclear targets at a time and taking into consideration the experimental technologies discussed previously, we have found that among all possible combinations the most stringent sensitivity corresponds to a combined measurement of $^{20}\text{Ne} + {}^{76}\text{Ge}$, which for the realistic (optimistic) case reads

TABLE IV. Expected sensitivities to the weak mixing angle $\sin^2\theta_W(\nu_\mu) \equiv s_W^2(\nu_\mu)$, through a combined analysis of the prompt and delayed beams $(\nu_\mu + \bar{\nu}_\mu)$. The same conventions as in Table III are used.

Nucleus	^{20}Ne	^{40}Ar	^{76}Ge	^{132}Xe
$\delta s_W^2(\nu_\mu)$	0.0052 [0.0007]	0.0042 [0.0006]	0.0031 [0.0005]	0.0073 [0.0004]
Uncertainty (%)	2.23 [0.30]	1.82 [0.26]	1.34 [0.22]	3.14 [0.17]

$$\mu_{\nu_\mu} = 6.48(1.77) \times 10^{-10}\mu_B \quad 90\%\ \text{C.L.} \tag{13}$$

The above sensitivity is better than the case with only one detector. Notice also that the optimistic sensitivity shown here gives an idea to the potential constraint that could be achieved by improving the experimental setup. Moreover, a combined measurement of all possible target nuclei would lead to somewhat better expected sensitivities, i.e.,

$$\mu_{\nu_\mu} = 5.87(1.52) \times 10^{-10}\mu_B \quad 90\%\ \text{C.L.} \tag{14}$$

Eventually, we explore the possibility of varying more than one parameter at the same time. To this aim, a χ^2 analysis is performed, but in this case the fitted parameters were simultaneously varied. Within this context, the contours of the $\sin^2\theta_W - \mu_\nu$ parameter space at 90% C.L. are illustrated in Fig. 5. Finally, in Fig. 6 the allowed regions of the parameter space in the $\mu_{\bar{\nu}_\mu} - \mu_{\nu_e}$ plane are shown, where the corresponding results have been evaluated at 90% C.L.

V. DISCUSSION AND CONCLUSIONS

We have studied the sensitivities on Majorana neutrino magnetic moments attainable through neutral current coherent neutrino-nucleus scattering cross section calculations at the Spallation Neutron Source. Regarding the meaning of the parameter μ_{eff} describing the effective neutrino magnetic moment, in general this can be expressed through neutrino amplitudes of positive and negative helicity states (which we denote as the 3-vectors a_+ and a_-, respectively) and the magnetic moment matrix, λ. Within this notation, the effective neutrino magnetic moment reads [23]

$$\mu_{\text{eff}}^2 = a_+^\dagger \lambda \lambda^\dagger a_+ + a_-^\dagger \lambda \lambda^\dagger a_-. \tag{15}$$

In this work, we mainly focus on the muon-neutrino signal. Then, considering the muon neutrino as having a Majorana nature, we have, in the flavor basis

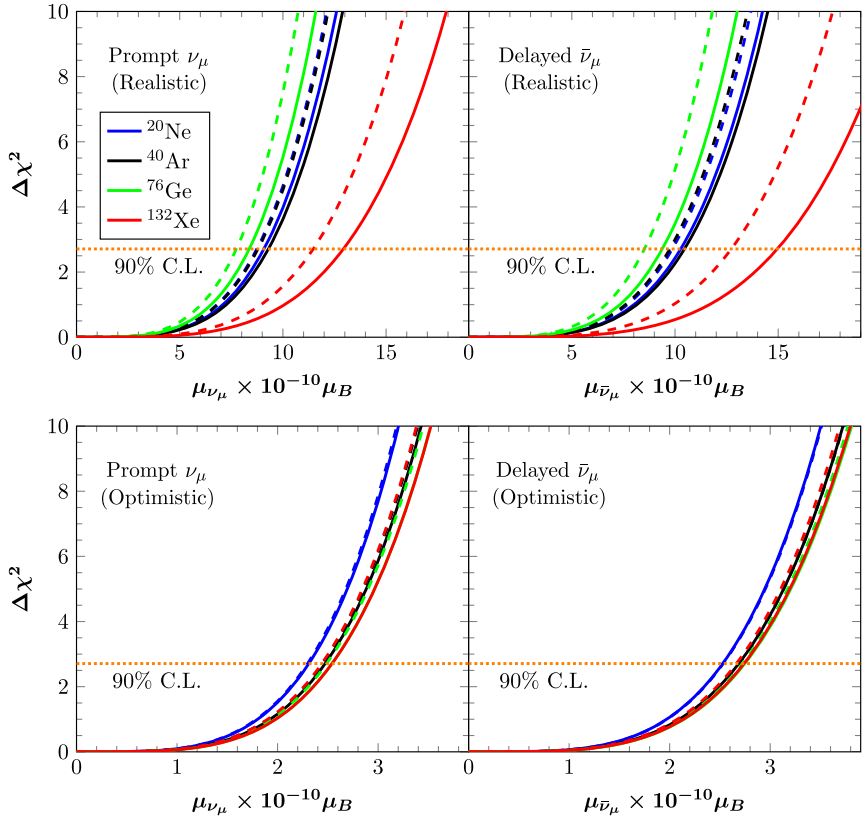

FIG. 3 (color online). $\Delta\chi^2$ profiles for a neutrino magnetic moment, μ_{ν_μ} in units of $10^{-10}\mu_B$, of the COHERENT experiment, assuming various nuclear detectors. The same conventions as in Fig. 1 are used.

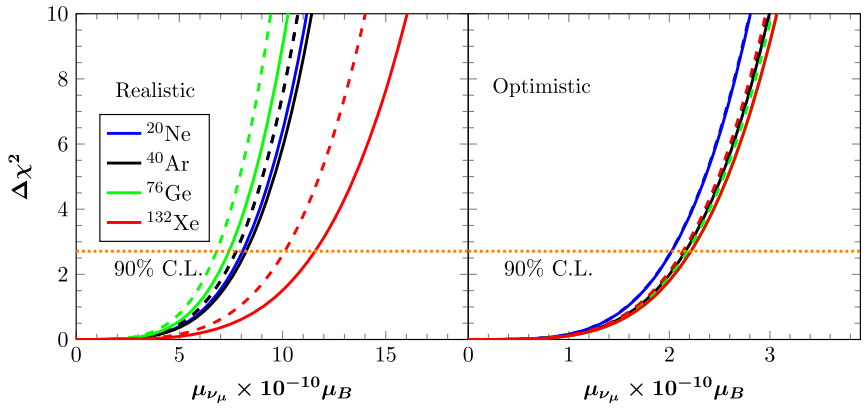

FIG. 4 (color online). $\Delta\chi^2$ profile for a neutrino magnetic moment, μ_{ν_μ}, in units of $10^{-10}\mu_B$, from the combined measurement of the prompt and delayed beams ($\nu_\mu + \bar{\nu}_\mu$). The same conventions as in Fig. 1 are used.

$$\mu^2_{\text{eff}} = |\Lambda_e|^2 + |\Lambda_\tau|^2, \tag{16}$$

with $|\Lambda_e|$ and $|\Lambda_\tau|$ being the elements of the neutrino transition magnetic moment matrix λ describing the corresponding transitions from the muon neutrino to the tau and electron antineutrino states, respectively. The latter expression can be translated into the mass basis through a rotation by using the leptonic mixing matrix. An analogous expression can be found for purely electron neutrino states, for example. One can see that the limits on the effective neutrino magnetic moment obtained from neutrino experiments are in reality a restriction on a combination of physical observables. In this sense, an improvement in the muon effective neutrino magnetic

TABLE V. Upper limits on the neutrino magnetic moment (in units of $10^{-10}\mu_B$) at 90% C.L. expected at the COHERENT experiment for the realistic (optimistic) case. The results indicated with ($^{\text{comb}}$) are obtained from a combined measurement of the prompt and delayed beams.

Nucleus	^{20}Ne	^{40}Ar	^{76}Ge	^{132}Xe
μ_{ν_μ}	9.09 [2.31]	9.30 [2.47]	8.37 [2.54]	12.94 [2.54]
$\mu_{\bar{\nu}_\mu}$	10.28 [2.53]	10.46 [2.69]	9.39 [2.75]	14.96 [2.74]
μ_{ν_e}	10.22 [2.44]	10.55 [2.60]	9.46 [2.68]	15.20 [2.68]
$\mu_{\nu_\mu}^{\text{comb}}$	8.07 [2.02]	8.24 [2.16]	7.41 [2.22]	11.58 [2.21]

moment will contribute towards improving the constraints on the physical observables through a combined analysis of neutrino data. A full description of this formalism can be found in Ref. [23].

The sensitivities we have extracted are obtained by means of a simple χ^2 analysis employing realistic nuclear structure calculations within the QRPA, for the evaluation of the coherent cross section. We find that current limits on the muon-neutrino magnetic moment, μ_{ν_μ}, can be improved by half an order of magnitude. In addition, we show that the SNS allows for a competitive determination of the electroweak mixing angle θ_W. Moreover, the COHERENT proposal may provide an excellent probe for investigating other electromagnetic neutrino properties, such as the neutrino charge radius (see the Appendix). In view of the operation of proposed sensitive neutrino experiments (e.g., COHERENT) our results, presented for various choices of experimental setups and target materials, may contribute towards a deeper understanding of so-far hidden neutrino properties.

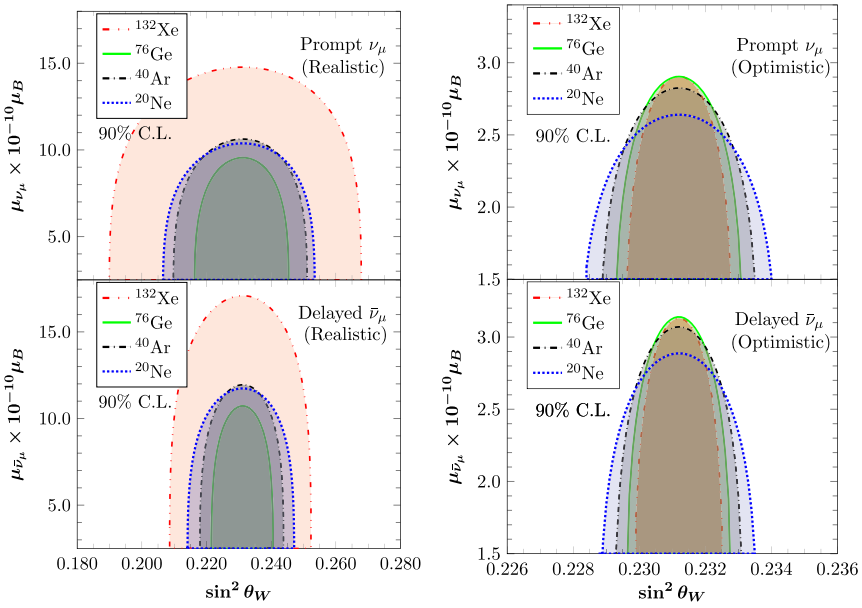

FIG. 5 (color online). The $\mu_{\nu_\mu}(\mu_{\bar{\nu}_\mu})$-$\sin^2\theta_W$ contours obtained from a two parameter χ^2 analysis. Allowed regions are shown for 90% C.L. Left (right) panels account for the realistic (optimistic) case, while the upper (lower) panels refer to the prompt (delayed) flux.

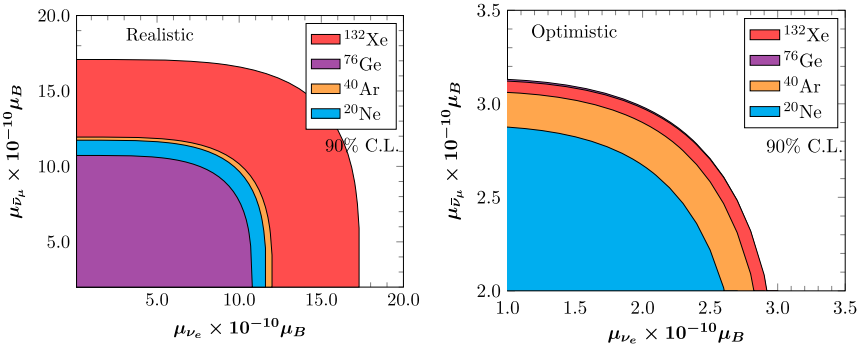

FIG. 6 (color online). The $\mu_{\bar{\nu}_\mu}$-μ_{ν_e} contours obtained from a two parameter χ^2 analysis. Allowed regions are shown for 90% C.L. Left (right) panel accounts for the realistic (optimistic) case.

ACKNOWLEDGMENTS

This work was supported by Spanish MINECO under Grants FPA2014-58183-P and MULTIDARK CSD2009-00064 (Consolider-Ingenio 2010 Programme), EPLANET, the CONACyT Grant No. 166639 (Mexico), and the Generalitat Valenciana Grant No. PROMETEOII/2014/084. D. K. P. was supported by "Prometeu per a grups d' investigació d' Excel lència de la Consellería d' Educació, Cultura i Esport, CPI-14-289" (Grant No. GVPROMETEOII2014-084). D. K. P. is grateful to Dr. Athanasios Hatzikoutelis for stimulating discussions. M. T. is also supported by a Ramon y Cajal contract of the Spanish MINECO.

APPENDIX Sensitivity to the Neutrino Charge Radius

Apart from the neutrino magnetic moment, the neutrino charge radius is another interesting electromagnetic property to be considered. In general, the electric form factor

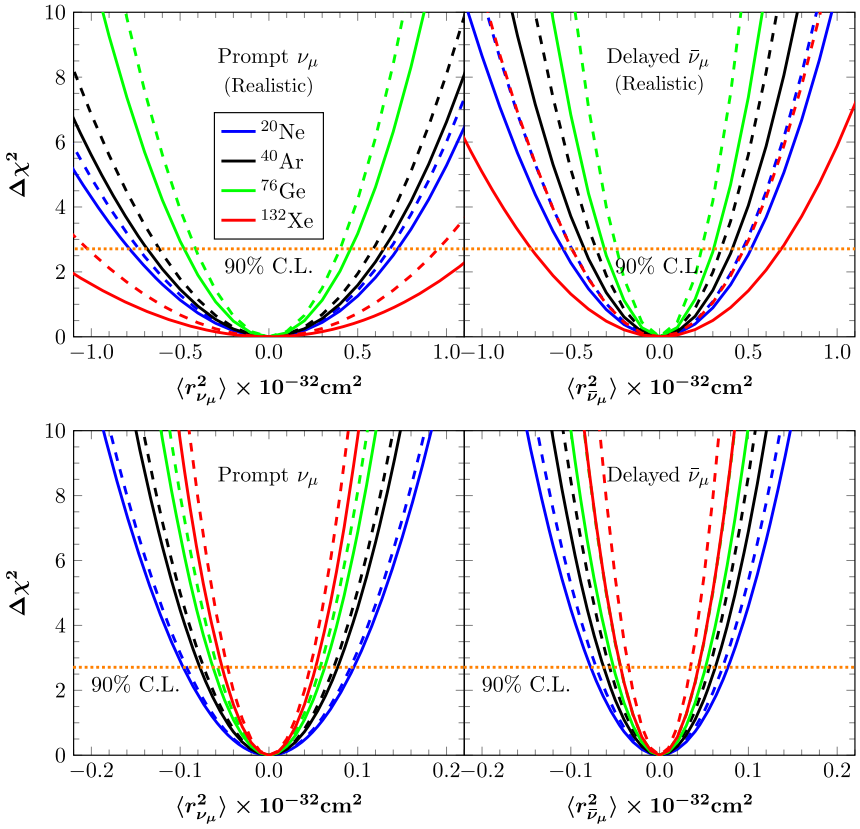

FIG. 7 (color online). $\Delta\chi^2$ profiles for a neutrino charge radius, $\langle r^2_{\nu_\mu}\rangle$ in units of 10^{-32} cm^2, of the COHERENT experiment, assuming various nuclear detectors. Same conventions as in Fig. 1 are used.

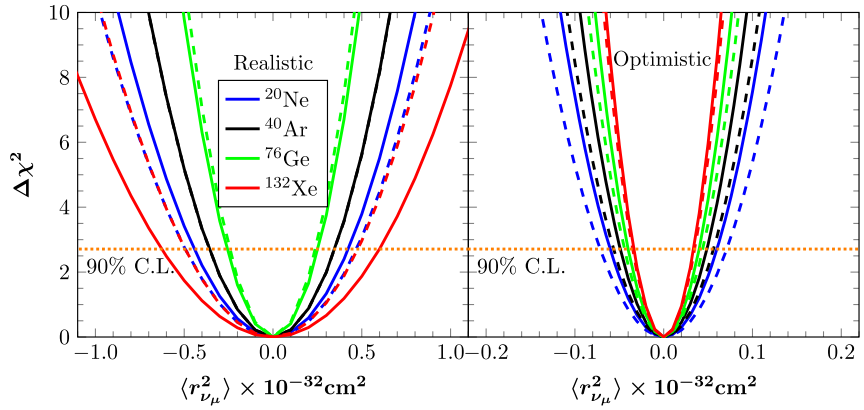

FIG. 8 (color online). $\Delta\chi^2$ profile for the neutrino charge radius, $\langle r^2_{\nu_\mu}\rangle$ in units of 10^{-32} cm^2, from the combined measurement of the prompt and delayed beams ($\nu_\mu + \bar{\nu}_\mu$). Same conventions as in Fig. 1 are used.

TABLE VI. Expected sensitivities on the neutrino charge radius (in units of 10^{-32} cm^2) from the analysis of the COHERENT experiment. The limits are presented at 90% C.L. for the realistic (optimistic) case. The results indicated with ($^{\text{comb}}$) are obtained from a combined measurement of the prompt and delayed beams.

Nucleus	^{20}Ne	^{40}Ar	^{76}Ge	^{132}Xe
$\langle r^2_{\bar{\nu}_\mu} \rangle$	−0.55–0.52 [−0.08–0.08]	−0.43–0.41 [−0.06–0.06]	−0.31–0.30 [−0.05–0.05]	−0.72–0.69 [−0.04–0.04]
$\langle r^2_{\nu_\mu} \rangle$	−0.79–0.73 [−0.10–0.10]	−0.69–0.65 [−0.08–0.08]	−0.48–0.46 [−0.06–0.06]	−1.31–1.20 [−0.05–0.05]
$\langle r^2_{\nu_e} \rangle$	−0.65–0.61 [−0.09–0.09]	−0.53–0.50 [−0.07–0.07]	−0.38–0.37 [−0.06–0.06]	−0.90–0.85 [−0.05–0.05]
$\langle r^2_{\nu_\mu} \rangle^{\text{comb}}$	−0.44–0.42 [−0.06–0.06]	−0.36–0.35 [−0.05–0.05]	−0.26–0.26 [−0.04–0.04]	−0.63–0.60 [−0.03–0.03]

allows us to extract nontrivial information concerning the neutrino electric properties, despite its neutral electric charge [12]. In fact, the gauge-invariant definition of the neutrino effective charge radius $\langle r^2_{\nu_\alpha} \rangle$, $\alpha = e, \mu, \tau$ was proposed long ago [21,22] as a physical observable related to the vector and axial vector form factors involving the EM interaction of a Dirac neutrino [8,26]. In particular, at the one-loop approximation a correction of a few percent to the weak mixing angle has been obtained [18–20],

$$\sin^2\theta_W \to \sin^2\overline{\theta_W} + \frac{\sqrt{2}\pi\alpha_{\text{em}}}{3G_F}\langle r^2_{\nu_\alpha} \rangle. \tag{A1}$$

Through CENNS, we estimate for the first time the sensitivity of a low energy SNS experiment to constrain the neutrino charge radius. The obtained bounds are derived in the context of a χ^2 analysis in the same spirit of the discussion made above and they are presented in Figs. 7–8 and listed in Table VI. As expected, the results behave similarly to the case of the weak mixing angle; thus we conclude that for the realistic (optimistic) case a 100 kg ^{76}Ge (heavy ^{132}Xe) detector at 20 m is required to constrain more significantly the neutrino charge radius. Furthermore, through a combined measurement of the prompt and delayed beams ($\nu_\mu + \bar{\nu}_\mu$) an appreciably improved sensitivity can be reached for $\langle r^2_{\nu_\mu} \rangle$ in comparison to $\langle r^2_{\nu_e} \rangle$. These sensitivities are better than current ones (see Ref. [12] and references therein) and depending on the detector setup may improve by one order of magnitude.

[1] J. Schechter and J. Valle, Neutrino masses in SU(2) × U(1) theories, Phys. Rev. D **22**, 2227 (1980).

[2] J. Schechter and J. Valle, Neutrino decay and spontaneous violation of lepton number, Phys. Rev. D **25**, 774 (1982).

[3] M. Maltoni, T. Schwetz, M. Tortola, and J. W. F. Valle, Status of global fits to neutrino oscillations, New J. Phys. **6**, 122 (2004). This review gives a comprehensive set of references.

[4] H. Nunokawa, S. J. Parke, and J. W. Valle, *CP* violation and neutrino oscillations, Prog. Part. Nucl. Phys. **60**, 338 (2008).

[5] J. W. Valle and J. C. Romao, *Neutrinos in High Energy and Astroparticle Physics*, 1st ed. (Wiley-VCH, Berlin, 2015).

[6] S. M. Boucenna, S. Morisi, and J. W. Valle, The low-scale approach to neutrino masses, Adv. High Energy Phys. **2014**, 831598 (2014).

[7] J. Schechter and J. W. F. Valle, Majorana neutrinos and magnetic fields, Phys. Rev. D **24**, 1883 (1981); **25**, 283(E) (1982).

[8] R. E. Shrock, Electromagnetic properties and decays of Dirac and Majorana neutrinos in a general class of gauge theories, Nucl. Phys. **B206**, 359 (1982).

[9] B. Kayser, Majorana neutrinos and their electromagnetic properties, Phys. Rev. D **26**, 1662 (1982).

[10] J. F. Nieves, Electromagnetic properties of Majorana neutrinos, Phys. Rev. D **26**, 3152 (1982).

[11] J. F. Beacom and P. Vogel, Neutrino Magnetic Moments, Flavor Mixing, and the Super-Kamiokande Solar Data, Phys. Rev. Lett. **83**, 5222 (1999).

[12] C. Broggini, C. Giunti, and A. Studenikin, Electromagnetic properties of neutrinos, Adv. High Energy Phys. **2012**, 459526 (2012).

[13] D. Forero, M. Tortola, and J. W. F. Valle, Global status of neutrino oscillation parameters after recent reactor measurements, Phys. Rev. D **86**, 073012 (2012).

[14] D. Forero, M. Tortola, and J. Valle, Neutrino oscillations refitted, Phys. Rev. D **90**, 093006 (2014).

[15] J. Beringer *et al.* (Particle Data Group Collaboration), Review of particle physics (RPP), Phys. Rev. D **86**, 010001 (2012).
[16] O. G. Miranda, T. I. Rashba, A. I. Rez, and J. W. F. Valle, Constraining the Neutrino Magnetic Moment with Antineutrinos from the Sun, Phys. Rev. Lett. **93**, 051304 (2004).
[17] O. G. Miranda, T. I. Rashba, A. I. Rez, and J. W. F. Valle, Enhanced solar antineutrino flux in random magnetic fields, Phys. Rev. D **70**, 113002 (2004).
[18] M. Hirsch, E. Nardi, and D. Restrepo, Bounds on the tau and muon-neutrino vector and axial vector charge radius, Phys. Rev. D **67**, 033005 (2003).
[19] J. Bernabeu, L. Cabral-Rosetti, J. Papavassiliou, and J. Vidal, On the charge radius of the neutrino, Phys. Rev. D **62**, 113012 (2000).
[20] J. Barranco, O. Miranda, and T. Rashba, Improved limit on electron neutrino charge radius through a new evaluation of the weak mixing angle, Phys. Lett. B **662**, 431 (2008).
[21] W. A. Bardeen, R. Gastmans, and B. Lautrup, Static quantities in Weinberg's model of weak and electromagnetic interactions, Nucl. Phys. **B46**, 319 (1972).
[22] S. Lee, Higher-order corrections to leptonic processes and the renormalization of Weinberg's theory of weak interactions in the unitary gauge, Phys. Rev. D **6**, 1701 (1972).
[23] W. Grimus, M. Maltoni, T. Schwetz, M. A. Tortola, and J. W. F. Valle, Constraining Majorana neutrino electromagnetic properties from the LMA-MSW solution of the solar neutrino problem, Nucl. Phys. **B648**, 376 (2003).
[24] M. A. Tortola, Constraining neutrino magnetic moment with solar and reactor neutrino data, *Proc. Sci.*, AHEP2003 (2003) 022 [arXiv:hep-ph/0401135].
[25] B. W. Lee and R. E. Shrock, Natural suppression of symmetry violation in gauge theories: muon-lepton and electron lepton number nonconservation, Phys. Rev. D **16**, 1444 (1977).
[26] P. Vogel and J. Engel, Neutrino electromagnetic form factors, Phys. Rev. D **39**, 3378 (1989).
[27] M. Czakon, J. Gluza, and M. Zralek, Neutrino magnetic moments in left-right symmetric models, Phys. Rev. D **59**, 013010 (1998).
[28] A. Povarov, Scalar-leptoquark contributions to the neutrino magnetic moment, Phys. At. Nucl. **70**, 871 (2007).
[29] M. Gozdz, Constraining an R-parity violating supergravity model with the Higgs induced Majorana neutrino magnetic moments, Phys. Rev. D **85**, 055016 (2012).
[30] R. Mohapatra, S.-P. Ng, and H.-b. Yu, Reactor searches for neutrino magnetic moment as a probe of extra dimensions, Phys. Rev. D **70**, 057301 (2004).
[31] G. G. Raffelt, Limits on neutrino electromagnetic properties: an update, Phys. Rep. **320**, 319 (1999).
[32] N. Viaux, M. Catelan, P. B. Stetson, G. G. Raffelt, J. Redondo, A. A. R. Valcarce, and A. Weiss, Neutrino and Axion Bounds from the Globular Cluster m5 (ngc 5904), Phys. Rev. Lett. **111**, 231301 (2013).
[33] L. B. Auerbach *et al.* (LSND Collaboration), Measurement of electron-neutrino electron elastic scattering, Phys. Rev. D **63**, 112001 (2001).
[34] R. Allen, H. Chen, P. Doe, R. Hausammann, W. Lee *et al.*, Study of electron-neutrino electron elastic scattering at LAMPF, Phys. Rev. D **47**, 11 (1993).
[35] H. Wong *et al.* (TEXONO Collaboration), A search of neutrino magnetic moments with a high-purity Germanium detector at the Kuo-Sheng nuclear power station, Phys. Rev. D **75**, 012001 (2007).
[36] A. G. Beda, V. B. Brudanin, V. G. Egorov, D. V. Medvedev, V. S. Pogosov, M. V. Shirchenko, and A. S. Starostin, The results of search for the neutrino magnetic moment in GEMMA experiment, Adv. High Energy Phys. **2012**, 350150 (2012).
[37] D. Z. Freedman, Coherent neutrino-nucleus scattering as a probe of the weak neutral current, Phys. Rev. D **9**, 1389 (1974).
[38] A. Drukier and L. Stodolsky, Principles and applications of a neutral current detector for neutrino physics and astronomy, Phys. Rev. D **30**, 2295 (1984).
[39] O. G. Miranda, M. A. Tortola, and J. W. F. Valle, Are solar neutrino oscillations robust? J. High Energy Phys. 10 (2006) 008.
[40] K. Scholberg, Prospects for measuring coherent neutrino-nucleus elastic scattering at a stopped-pion neutrino source, Phys. Rev. D **73**, 033005 (2006).
[41] J. Barranco, O. Miranda, and T. Rashba, Probing new physics with coherent neutrino scattering off nuclei, J. High Energy Phys. 12 (2005) 021.
[42] J. Barranco, O. G. Miranda, C. A. Moura, and J. W. F. Valle, Constraining nonstandard interactions in nu/e e or anti nu/e e scattering, Phys. Rev. D **73**, 113001 (2006).
[43] J. Barranco, O. Miranda, and T. Rashba, Low energy neutrino experiments sensitivity to physics beyond the standard model, Phys. Rev. D **76**, 073008 (2007).
[44] F. J. Escrihuela, O. G. Miranda, M. A. Tortola, and J. W. F. Valle, Constraining nonstandard neutrino-quark interactions with solar, reactor, and accelerator data, Phys. Rev. D **80**, 105009 (2009).
[45] F. J. Escrihuela, M. Tortola, J. W. F. Valle, and O. G. Miranda, Global constraints on muon-neutrino nonstandard interactions, Phys. Rev. D **83**, 093002 (2011).
[46] T. Kosmas, J. Vergados, O. Civitarese, and A. Faessler, Study of the muon number violating (mu-, e-) conversion in a nucleus by using quasiparticle RPA, Nucl. Phys. **A570**, 637 (1994).
[47] T. S. Kosmas, Exotic mu- → e- conversion in nuclei: energy moments of the transition strength and average energy of the outgoing e-, Nucl. Phys. **A683**, 443 (2001).
[48] D. Papoulias and T. Kosmas, Exotic lepton flavor violating processes in the presence of nuclei, J. Phys. Conf. Ser. **410**, 012123 (2013).
[49] D. Papoulias and T. Kosmas, Nuclear aspects of neutral current nonstandard ν-nucleus reactions and the role of the exotic $\mu^- \to e^-$ transitions experimental limits, Phys. Lett. B **728**, 482 (2014).
[50] D. Papoulias and T. Kosmas, Standard and nonstandard neutrino-nucleus reactions cross sections and event rates to neutrino detection experiments, Adv. High Energy Phys. **2015**, 763648 (2014).
[51] T. Donnelly and J. Walecka, Semileptonic weak and electromagnetic interactions with nuclei: isoelastic processes, Nucl. Phys. **A274**, 368 (1976).

[52] V. Chasioti and T. Kosmas, A unified formalism for the basic nuclear matrix elements in semileptonic processes, Nucl. Phys. **A829**, 234 (2009).
[53] P. Giannaka and T. Kosmas, Electron capture and its role in explosive neutrino nucleosynthesis, J. Phys. Conf. Ser. **410**, 012124 (2013).
[54] P. Giannaka and T. Kosmas, Electron capture cross sections for stellar nucleosynthesis, Adv. High Energy Phys. **2015**, 398796 (2015).
[55] A. Bolozdynya, F. Cavanna, Y. Efremenko, G. Garvey, V. Gudkov *et al.*, Opportunities for neutrino physics at the Spallation Neutron Source: a White paper, arXiv:1211.5199.
[56] D. Akimov *et al.* (CSI Collaboration), Coherent scattering investigations at the Spallation Neutron Source: a Snowmass White paper, arXiv:1310.0125.
[57] See the web site about "Neutrino Studies at the Spallation Neutron Source" at http://www.phy.ornl.gov/nusns.
[58] F. Avignone and Y. Efremenko, Neutrino-nucleus cross-section measurements at intense, pulsed spallation sources, J. Phys. G **29**, 2615 (2003).
[59] Y. Efremenko and W. Hix, Opportunities for neutrino physics at the Spallation Neutron Source (SNS), J. Phys. Conf. Ser. **173**, 012006 (2009).
[60] S. Brice, R. Cooper, F. DeJongh, A. Empl, L. Garrison *et al.*, A method for measuring coherent elastic neutrino-nucleus scattering at a far off-axis high-energy neutrino beam target, Phys. Rev. D **89**, 072004 (2014).
[61] J. I. Collar, N. E. Fields, M. Hai, T. W. Hossbach, J. L. Orrell, C. T. Overman, G. Perumpilly, and B. Scholz, Coherent neutrino-nucleus scattering detection with a CsI [Na] scintillator at the SNS spallation source, Nucl. Instrum. Methods Phys. Res., Sect. A **773**, 56 (2015).
[62] V. Chepel and H. Araújo, Liquid noble gas detectors for low energy particle physics, J. Instrum. **8**, R04001 (2013).
[63] A. Aguilar-Arevalo *et al.* (MiniBooNE Collaboration), The neutrino flux prediction at MiniBooNE, Phys. Rev. D **79**, 072002 (2009).
[64] W. Louis, Searches for muon-to-electron (anti) neutrino flavor change, Prog. Part. Nucl. Phys. **63**, 51 (2009).
[65] P. Amanik and G. McLaughlin, Nuclear neutron form factor from neutrino-nucleus coherent elastic scattering, J. Phys. G **36**, 015105 (2009).
[66] K. Scholberg, T. Wongjirad, E. Hungerford, A. Empl, D. Markoff *et al.*, The CLEAR experiment, arXiv:0910.1989.
[67] A. Soma *et al.* (TEXONO Collaboration), Extraction of physics signals near threshold with Germanium detectors in neutrino and dark matter experiments, arXiv:1411.4802.
[68] J. Yoo, http://if-neutrino.fnal.gov/neutrino1-pagers.pdf, 2011.
[69] A. J. Anderson, J. M. Conrad, E. Figueroa-Feliciano, C. Ignarra, G. Karagiorgi, K. Scholberg, M. H. Shaevitz, and J. Spitz, Measuring active-to-sterile neutrino oscillations with neutral current coherent neutrino-nucleus scattering, Phys. Rev. D **86**, 013004 (2012).
[70] D. Papoulias and T. Kosmas, Neutrino transition magnetic moments within the non-standard neutrino-nucleus interactions, arXiv:1506.05406 [Phys. Lett. B (to be published)].